Acta Cryst. (1999). B**55**, 306–312

Structures of $Bi_{14}WO_{24}$ and $Bi_{14}MoO_{24}$ from neutron powder diffraction data

Christopher D. Ling,* Ray L. Withers, John G. Thompson and Siegbert Schmid

Research School of Chemistry, Australian National University, Canberra, ACT 0200, Australia.
E-mail: ling@rsc.anu.edu.au

(*Received 9 June 1998; accepted 27 October 1998*)

Abstract

The (isomorphous) structures of $Bi_{14}WO_{24}$, tetradecabismuth tungsten tetracosaoxide, and $Bi_{14}MoO_{24}$, tetradecabismuth molybdenum tetracosaoxide, have been solved and refined using neutron powder diffraction data in the space group $I4/m$. The metal-atom array is fully ordered in terms of composition, and in terms of atomic positions deviates only slightly from a fluorite-type δ-Bi_2O_3-related parent structure. Three independent O-atom sites (accounting for 70 out of 78 O atoms in the unit cell) are also very close to fluorite-type parent positions. The remaining two O-atom sites, which coordinate W, exhibit partial occupancies and displacive disorder, neither of which could be better modelled by lowering of symmetry. The W site is coordinated by four O atoms in highly distorted tetrahedral coordination, the tetrahedron necessarily being orientationally disordered on that site. Nonetheless, the structure appears to be chemically reasonable.

1. Introduction

$Bi_{14}WO_{24}$ and $Bi_{14}MoO_{24}$ are examples of bismuth-rich phases in binary oxide systems which appear to form modulated structures preserving the average structure of δ-Bi_2O_3 (Zhou, 1994, Ling *et al.*, 1998). Interest in such phases stems from an inability to quench the high-temperature phase δ-Bi_2O_3 to room temperature. δ-Bi_2O_3 is one of the best oxygen-ion conductors known (Takahashi & Iwahara, 1978; Sleight, 1980). It is reported as a fluorite-type structure with 25% average oxygen vacancies (Gattow & Schröder, 1962; Harwig, 1978), the approximate preservation of which is thought to be responsible for the preservation of anionic conduction properties in such bismuth-rich binary oxide phases (Allnat & Jacobs, 1961, 1967).

$Bi_{14}WO_{24}$ was described, in an electron diffraction (ED) study by Zhou (1994), as a 'type Ia' superstructure of fluorite-type δ-Bi_2O_3. In our recent reinvestigation of bismuth-rich phases in a number of binary oxide systems (Ling *et al.*, 1998), we reproduced Zhou's ED results for $Bi_{14}WO_{24}$ and found that $Bi_{14}MoO_{24}$ (Egashira *et al.*, 1979) appeared to have an isomorphous structure. For both phases, preliminary Rietveld refinement of metal-atom positions in Zhou's $I4/m$ model using synchrotron X-ray diffraction (XRD) data indicated that the metal-atom coordinates were indeed very close to a face-centred-cubic (f.c.c.) fluorite-type average. Zhou's model for O-atom positions lowers the symmetry from $I4/m$ to $I1$ (*i.e.* $P1$) by removal of selected O atoms (and their body-centred equivalents) from the model without displacing any remaining atoms from the fluorite-type average positions. We wished to investigate the structures of these phases in terms of both displacive and occupational modulations away from the fluorite-type parent structure.

Successful synthesis of $Bi_{14}WO_{24}$ and $Bi_{14}MoO_{24}$ as nearly single-phase powders on a sufficiently large scale has now allowed collection of time-of-flight (t.o.f.) neutron powder diffraction data. The greater relative contribution of O atoms to neutron diffraction intensities (compared with their contribution to X-ray diffraction intensities) has allowed us to model and refine O-atom parameters as well as those of the metal atoms. Here we report and discuss solutions for the (isomorphous) structures of $Bi_{14}WO_{24}$ and $Bi_{14}MoO_{24}$, solved and refined using neutron powder diffraction data.

2. Experimental

Powder samples of $Bi_{14}WO_{24}$ and $Bi_{14}MoO_{24}$ were prepared by solid-state reactions of stoichiometric mixtures of Bi_2O_3 (Koch–Lite 99.998%), WO_3 (Koch–Lite 99.9%) and MoO_3 (Halewood 99.999%) in platinum crucibles in air at 1103 K ($Bi_{14}WO_{24}$) or 1073 K ($Bi_{14}MoO_{24}$) for 0.5 h. The samples were then quenched to room temperature, reground, annealed in sealed platinum vessels at 1103 K ($Bi_{14}WO_{24}$) or 1073 K ($Bi_{14}MoO_{24}$) for 168 h and again quenched to room temperature. The use of sealed platinum vessels was found to be the best way of controlling the stoichiometry in face of the volatility of the reactants (Ling *et al.*, 1998). Homogeneous pale yellow powders were obtained and identified as predominantly single-phase $Bi_{14}WO_{24}$ and $Bi_{14}MoO_{24}$ by XRD (Jungner XDC-700 Guinier–Hägg camera) (Ling *et al.*, 1998). In neither case was it possible to eliminate small traces of a γ-Bi_2O_3-type phase (Harwig, 1978). This impurity was incorporated into both refinements using the model of

Table 1. *Experimental details*

Crystal data		
Chemical formula	$Bi_{14}WO_{24}$	$Bi_{14}MoO_{24}$
Chemical formula weight	3493.57	3405.66
Cell setting	Tetragonal	Tetragonal
Space group	*I*4/*m*	*I*4/*m*
a (Å)	8.71083 (4)	8.70839 (4)
c (Å)	17.32202 (10)	17.31634 (14)
V (Å^3)	1314.369 (11)	1313.202 (14)
Z	2	2
Radiation type	Neutron	Neutron
Temperature (K)	293	293
Specimen shape	Cylinder	Cylinder
Specimen size (mm)	30 × 15 × 15	25 × 8 × 8
Preparation conditions	101.3 kPa, 1103 K	101.3 kPa, 1073 K
Particle morphology	Plate	Plate
Colour	Yellow	Yellow
Data collection		
Diffractometer	HRPD and POLARIS	POLARIS
Detector	^{6}Li-doped glass scintillar (HRPD); ^{3}He gas and ZnS scintillation counters (POLARIS)	^{3}He gas and ZnS scintillation counters
Data collection method	Time-of-flight scans	Time-of-flight scans
Specimen mounting	Vanadium can	Vanadium can
Refinement		
R_p	0.0589	0.0387
R_{wp}	0.0605	0.0246
Profile function	Exponential pseudo-Voigt convolution (Von Dreele, 1990)	Exponential pseudo-Voigt convolution (Von Dreele, 1990)
No. of parameters used	56	56
Computer programs		
Structure refinement	*GSAS* (Larson & Von Dreele, 1991)	*GSAS* (Larson & Von Dreele, 1991)

Harwig (1978) and refining only the phase fraction. Although XRD data indicated the samples were highly homogenous, the presence of small impurities and the fact that Zhou (1994) reported a solid-solution between $Bi_{30}WO_{48}$ and $Bi_{14}WO_{24}$ meant that slight compositional inhomogeneities were possible.

Powder neutron diffraction data for $Bi_{14}MoO_{24}$ were collected on POLARIS (Hull *et al.*, 1992), the high-flux medium-resolution instrument at ISIS (Rutherford Appleton Laboratories, England). Data for $Bi_{14}WO_{24}$ were collected on the high-resolution powder diffractometer (HRPD) at the same facility (Ibberson *et al.*, 1992); supplementary high-*d* data for $Bi_{14}WO_{24}$ were collected on POLARIS. Experimental details for these diffraction experiments are summarized in Table 1 (POLARIS data for $Bi_{14}WO_{24}$ were collected under the same conditions as for $Bi_{14}MoO_{24}$).†

3. Refinement

3.1. *$Bi_{14}WO_{24}$*

The relationship between the unit cells of $Bi_{14}WO_{24}$ and fluorite-type δ-Bi_2O_3 determined by Zhou (1994) [$\mathbf{a} = \frac{3}{2}\mathbf{a}_f - \frac{1}{2}\mathbf{b}_f$, $\mathbf{b} = \frac{1}{2}\mathbf{a}_f + \frac{3}{2}\mathbf{b}_f$, $\mathbf{c} = 3\mathbf{c}_f$] was used to obtain a fluorite-type starting model for the structure of $Bi_{14}WO_{24}$. The W atom was placed on the origin in the space group *I*4/*m*, the highest symmetry in which it is possible to obtain the correct Bi:W ratio. Full occupancy of all fluorite-type O-atom positions gave this model a stoichiometry $Bi_{14}WO_{30}$. This corresponds to the initial oxygen-rich model of Zhou (1994).

Metal-atom coordinates were then shifted slightly according to the results of the preliminary Rietveld refinement of the model based on synchrotron X-ray data (see §1). This provided an initial phasing of the modulation of the true structure away from fluorite-type. Fixing the metal atoms and refining O-atom positional and U_{iso} parameters led to unstable refinements and rapid growth in the error estimates and U_{iso} parameters for two of the five independent O-atom sites. Removal of these two atoms from the model led to a very stable refinement in which it was possible to simultaneously refine metal-atom positional and U_{iso} parameters. The removed O atoms are those closest to W. This is an oxygen-poor model, $Bi_{14}WO_{20}$, in which W is clearly grossly underbonded.

Analysis of difference Fourier maps showed good agreement, except in the vicinity of the W atom, and led to the clear identification of two non-fluorite O atoms bonding to W, on the fourfold axis [O(1)] and on the

† Supplementary data for this paper are available from the IUCr electronic archives (Reference: OS0017). Services for accessing these data are described at the back of the journal.

mirror plane [O(3)]. These form the axial and equatorial O atoms, respectively, of a WO_6 octahedron. With full occupancy on both sites the stoichiometry is now again oxygen-rich, $Bi_{14}WO_{28}$. It was possible to refine positional and U_{iso} parameters for these atoms, resulting in a significant improvement in refinement statistics over the purely fluorite model; however, large error estimates and U_{iso} parameters for O(1) and O(3) indicated that this model did not represent a perfectly ordered solution. The nature of the disorder was investigated by fixing U_{iso} parameters for all O atoms to the same value and refining their occupancies. Occupancies for the fluorite-type O atoms were found to remain close to 1.0, while for O(1) and O(3) occupancies refined to approximately 0.5.

At this stage it was noted that the overall stoichiometry at which the material was synthesized, $Bi_{14}WO_{24}$, could be obtained with an occupancy for O(1) of 0.50 and for O(3) of 0.75, *i.e.* for each (average) WO_6 octahedron, one axial and one equatorial O atom would be vacant. Fixing the occupancies as such and freely refining all positional and U_{iso} parameters did indeed lead to the best refinement statistics obtained so far.

Refinement of anisotropic atomic displacement parameters for O(1) and O(3) showed that the motion of these atoms was predominantly perpendicular to the W—O bonds. Refinement of anisotropic atomic displacement parameters for the remaining atoms did not yield sufficient improvements in refinement statistics to justify the increased number of variables. Consideration was also given to the possibility of correlation between atomic displacement parameters and other variables in Rietveld refinements, in particular absorption; clearly, however, the magnitude of the anisotropies observed for O(1) and O(3) makes it unlikely that these are artefacts.

A series of attempts were made to find a fully ordered solution for the structure in lower-symmetry space groups. The tetrahedral space groups $I\bar{4}$ and $I4$, and the monoclinic space group $I2/m$, were tried without success. In all cases, the refinements became less stable but the positions of O(1) and O(3) did not deviate significantly from the previously refined $I4/m$ positions. Removing O(1) and O(3) from the model, refining the remainder of the structure and reinvestigating the difference Fourier map led to the identification of the same sites. In $I\bar{4}$ and $I2/m$, compatible with fully ordered WO_4 tetrahedra,

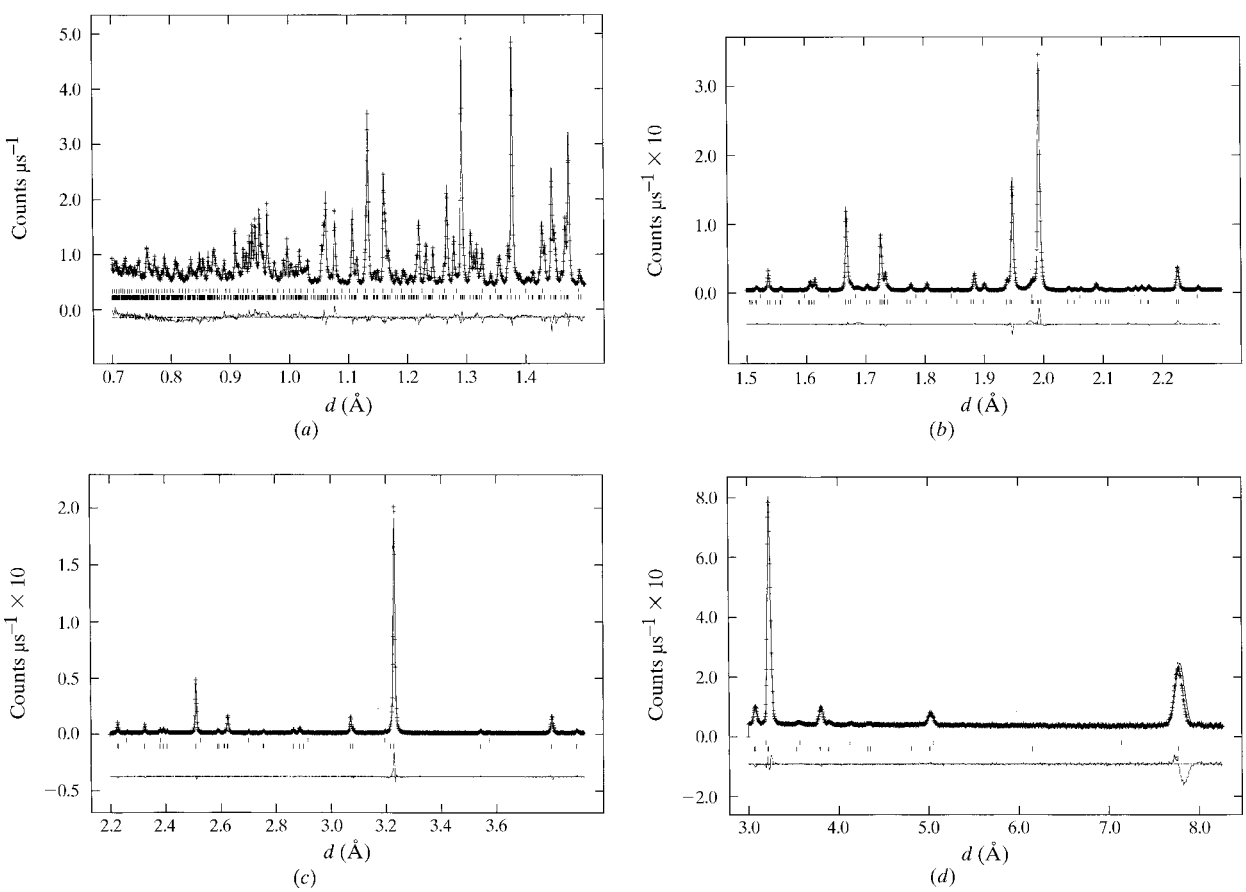

Fig. 1. Observed (+), calculated and difference (bottom) neutron powder diffraction profiles for $Bi_{14}WO_{24}$ using (*a*, *b*) 30–130 ms, (*c*) 100–200 ms t.o.f. windows with the backscattering detector of HRPD (Ibberson *et al.*, 1992) and (*d*) at the 145° detector bank of POLARIS (Hull *et al.*, 1992). The top row of reflection markers refers to the δ-Bi_2O_3-type impurity.

Table 2. *Structural parameters for the final Rietveld-refined structure of $Bi_{14}WO_{24}$*

O(1) and O(3) were refined anisotropically.

$$U_{eq} = (1/3)\Sigma_i\Sigma_j U^{ij} a^i a^j \mathbf{a}_i.\mathbf{a}_j.$$

	x	y	z	Fraction	$U_{iso}/U_{eq} \times 100$ (Å^2)
Bi(1)	0.43964 (20)	0.21318 (24)	0	1.0	1.75 (5)
Bi(2)	0.39520 (17)	0.20044 (20)	0.32999 (8)	1.0	1.451 (29)
Bi(3)	0	0	0.34328 (18)	1.0	3.13 (10)
W(1)	0	0	0	1.0	3.98 (24)
O(1)	0	0	0.1160 (5)	0.5	3.937
O(2)	0	1/2	0.12133 (23)	1.0	2.41 (7)
O(3)	0.1937 (9)	0.0173 (14)	0	0.75	19.359
O(4)	0.62577 (26)	0.31937 (24)	0.07821 (14)	1.0	2.28 (5)
O(5)	0.25407 (25)	0.07408 (22)	0.25610 (12)	1.0	2.33 (5)

	$U^{11} \times 100$ (Å^2)	$U^{22} \times 100$ (Å^2)	$U^{33} \times 100$ (Å^2)	$U^{12} \times 100$ (Å^2)	U^{13},$U^{23} \times 100$ (Å^2)
O(1)	5.0 (4)	5.0 (4)	1.7 (5)	0	0
O(3)	4.2 (5)	30.9 (15)	23.0 (12)	−4.7 (6)	0

attempts to constrain O atoms around W into such tetrahedra produced unstable refinements with poor statistics.

The validity of the initial phasing of the refinement in *I*4/*m* was investigated by returning all atoms to fluorite positions and refining the positions of O atoms before those of metal atoms. The same result was obtained, *i.e.* O atoms phase metal atoms and *vice versa*. Therefore, the refinement was not biased initially by the use of X-ray-refined metal-atom positions. It was concluded

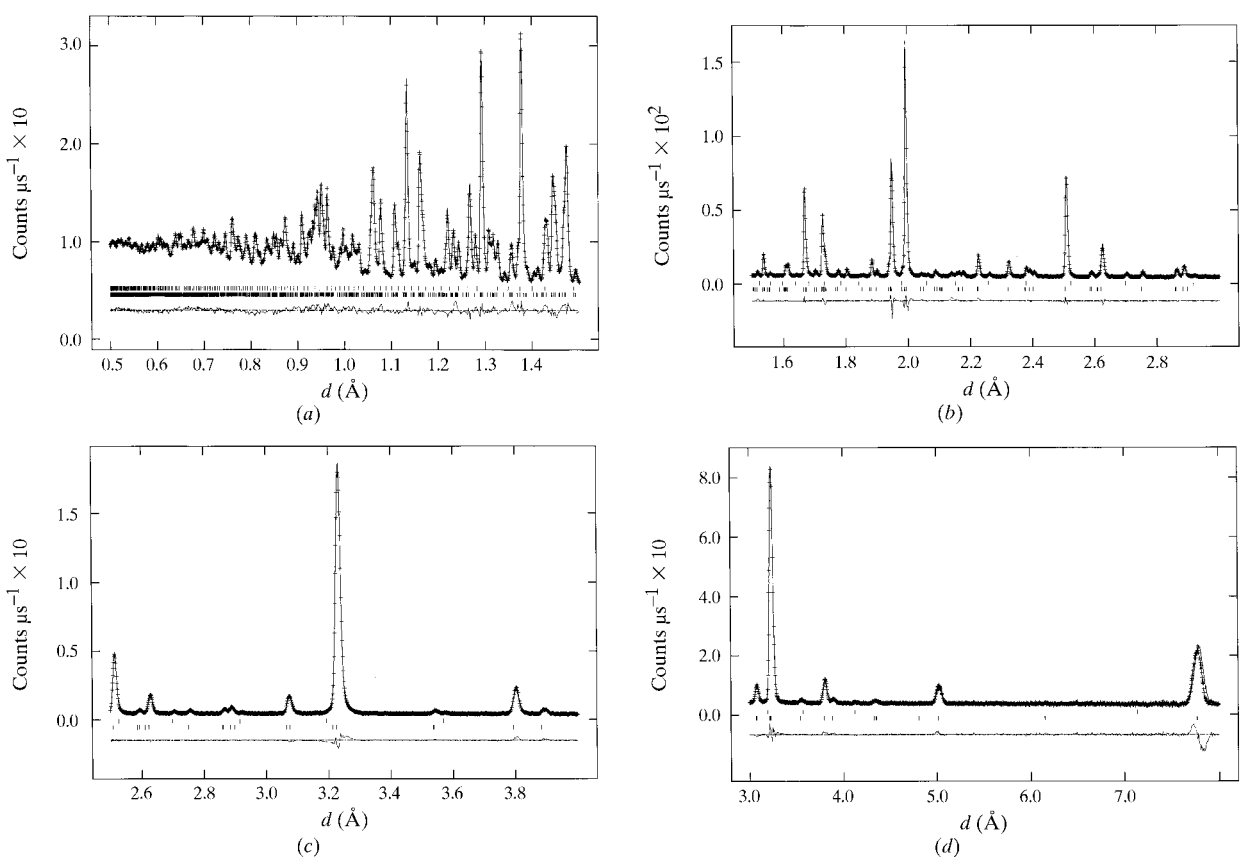

Fig. 2. Observed (+), calculated and difference (bottom) neutron powder diffraction profiles for $Bi_{14}MoO_{24}$ at the (*a*, *b*) 90, (*c*) 35 and (*d*) 145° detector banks of POLARIS (Hull *et al.*, 1992). The top row of reflection markers refers to the δ-Bi_2O_3-type impurity.

that none of the symmetry-lowering possibilities investigated resulted in sufficient deviations from the high-symmetry case to justify the additional degrees of freedom. The disordered *I*4/*m* model appeared to fit all observable data, reflecting disorder in the true structure.

Final refined values for the structural parameters are given in Table 2. Rietveld refinement statistics are summarized in Table 4. The refinement residuals for $Bi_{14}WO_{24}$, in particular $R(F^2)$, are in general higher than for $Bi_{14}MoO_{24}$, refined (§3.2) using lower-resolution data. This tendency for higher-resolution data to give apparently worse refinement statistics (but better results) is a consequence of the weighting scheme used in the Rietveld method. The final observed, calculated and difference powder neutron diffraction profiles are shown in Fig. 1.

3.2. *$Bi_{14}MoO_{24}$*

The final structure of $Bi_{14}WO_{24}$ was used as a starting model for the Rietveld refinement of POLARIS data for $Bi_{14}MoO_{24}$. The refinement rapidly converged from this starting model to a final refined structure which was clearly isomorphous with that of $Bi_{14}WO_{24}$. Final refined values for the structural parameters are given in Table 3. Rietveld-refinement statistics are summarized in Table 4. The final observed, calculated and difference powder neutron diffraction profiles are shown in Fig. 2.

4. Discussion

The final refined structure of $Bi_{14}WO_{24}$ is shown in Fig. 3. That of $Bi_{14}MoO_{24}$ is completely isomorphous. Figs. 3(*b*) and (*c*) are projections along the fluorite subcell directions according to the relationship described by Zhou (1994). The metal-atom array can be seen to closely preserve the f.c.c. arrangement of the fluorite-type subcell. It is also clear that the O-atom array only deviates significantly from fluorite in the immediate vicinity of W atoms, *i.e.* O(1) and O(3) are essentially the only non-fluorite-type O atoms in the structure. These sites between them account for only 8 atoms out of 78 in the unit cell, therefore the description of $Bi_{14}WO_{24}$ as a superstructure of fluorite-type δ-Bi_2O_3 is clearly valid.

With such a bismuth-rich composition, the coordination environments of the Bi atoms (Fig. 4) in $Bi_{14}WO_{24}$ may well be representative of those found in pure δ-Bi_2O_3. Discounting the long bonds to the non-fluorite-type O atoms O(1) and O(3), three different coordinations are seen to arise from the average cubic coordination of fluorite type: Bi(3) is surrounded by all eight O atoms of this cube, Bi(1) loses two adjacent O atoms from the cube to form a distorted trigonal prism and Bi(2) loses two adjacent and one opposite O atom from the cube to form a distorted square pyramid. The fact that all three have satisfactory calculated bond valences (Table 5), with the contributions of O(1) and O(3) being very small, indicates that all three sites should be plausible in δ-Bi_2O_3 itself.

In Fig. 3, WO_6 octahedra are depicted despite evidence from the refinement that only four out of six illustrated coordinating O atoms are, on average, present around each W atom. This suggests that the coordination environment of W is in fact distorted tetrahedral. Clearly, a tetrahedron formed from one axial and three equatorial O atoms of an average WO_6 octahedron would require serious local distortion to be chemically plausible. That such distortion occurs is evidenced by the extremely large anisotropic displacement parameters perpendicular to the W—O bonds for both O(1) and O(3) (Fig. 5).

The predominant motion of O(1) and O(3) perpendicular to W—O bonds is reasonable in terms of the bond-valence sums (Brese & O'Keeffe, 1991) calculated for the final refined structures and presented in Table 5. When the occupancies of the O(1) and O(3) sites are taken into account, the bond-valence requirements of W

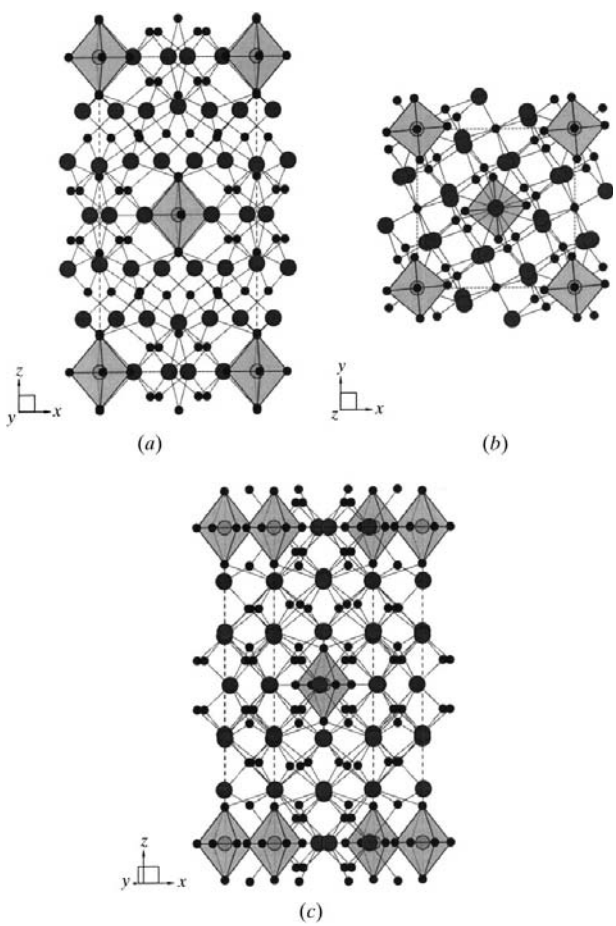

Fig. 3. The final refined structure of $Bi_{14}WO_{24}$ viewed down the (*a*) [010], (*b*) [001] and (*c*) [130] directions. WO_6 octahedra are shaded, Bi atoms are shown as large black spheres and O atoms as small black spheres.

Table 3. *Structural parameters for the final Rietveld-refined structure of $Bi_{14}MoO_{24}$*

O(1) and O(3) were refined anisotropically.

$$U_{eq} = (1/3)\Sigma_i\Sigma_j U^{ij} a^i a^j \mathbf{a}_i.\mathbf{a}_j.$$

	x	y	z	Fraction	$U_{iso}/U_{eq} \times 100$ (Å^2)
Bi(1)	0.44022 (13)	0.21306 (15)	0	1.0	0.966 (23)
Bi(2)	0.39542 (11)	0.20048 (13)	0.32975 (5)	1.0	0.794 (11)
Bi(3)	0	0	0.34376 (13)	1.0	1.59 (4)
Mo(1)	0	0	0	1.0	4.95 (15)
O(1)	0	0	0.1189 (4)	0.5	2.643
O(2)	0	1/2	0.12306 (16)	1.0	1.76 (4)
O(3)	0.1929 (7)	−0.0106 (16)	0	0.75	19.787
O(4)	0.62344 (18)	0.32173 (17)	0.07786 (10)	1.0	1.571 (27)
O(5)	0.25313 (15)	0.07313 (15)	0.25669 (8)	1.0	1.083 (21)

	$U^{11} \times 100$ (Å^2)	$U^{22} \times 100$ (Å^2)	$U^{33} \times 100$ (Å^2)	$U^{12} \times 100$ (Å^2)	U^{13},$U^{23} \times 100$ (Å^2)
O(1)	3.35 (21)	3.35 (21)	1.23 (27)	0	0
O(3)	4.8 (5)	38.9 (15)	15.6 (8)	2.4 (7)	0

are fulfilled, *i.e.* no changes in W—O bond length are required for a WO_4 tetrahedron to be chemically plausible. Calculated bond-valence sums for Bi and O atoms in pseudo-fluorite-type positions are also very reasonable. The only significant problem indicated by the bond-valence sums is an apparent under-bonding of O(1). No explanation can be offered other than to reiterate that this is a feature of the average position of O(1), and not necessarily of its local position with respect to coordinating metal atoms.

The finding that the crystal structures of $Bi_{14}WO_{24}$ and $Bi_{14}MoO_{24}$ are partially disordered is in itself significant. Their diffraction patterns contain large numbers of supercell reflections in addition to the

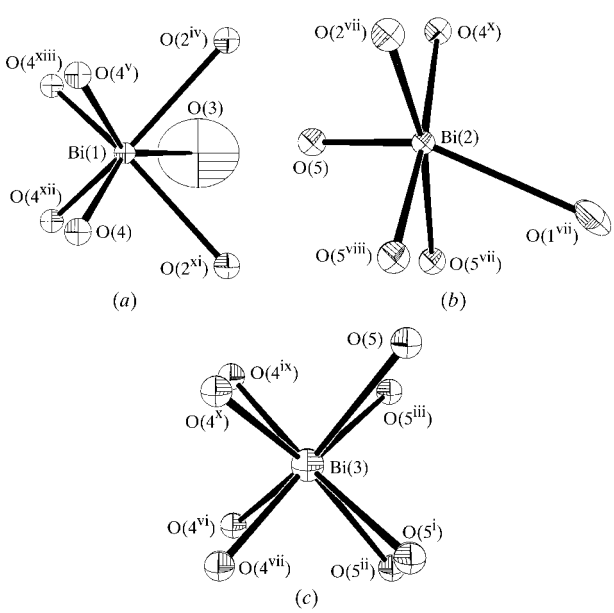

Fig. 4. *ORTEP*-3 (Farrugia, 1998) plots (ellipsoid probability 50%) showing the coordination environments of (*a*) Bi(1), (*b*) Bi(2) and (*c*) Bi(3) in the final refined structure of $Bi_{14}WO_{24}$. Symmetry codes: (i) $-y, x, z$; (ii) $-x, -y, z$; (iii) $y, -x, z$; (iv) $y, -x, -z$; (v) $x, y, -z$; (vi) $y-\frac{1}{2}, -x+\frac{1}{2}, -z+\frac{1}{2}$; (vii) $-x+\frac{1}{2}, -y+\frac{1}{2}, -z+\frac{1}{2}$; (viii) $y+\frac{1}{2}, -x+\frac{1}{2}, -z+\frac{1}{2}$; (ix) $x-\frac{1}{2}, y-\frac{1}{2}, -z+\frac{1}{2}$; (x) $-y+\frac{1}{2}, x-\frac{1}{2}, -z+\frac{1}{2}$; (xi) $1-y, x, z$; (xii) $y, 1-x, z$; (xiii) $y, 1-x, -z$.

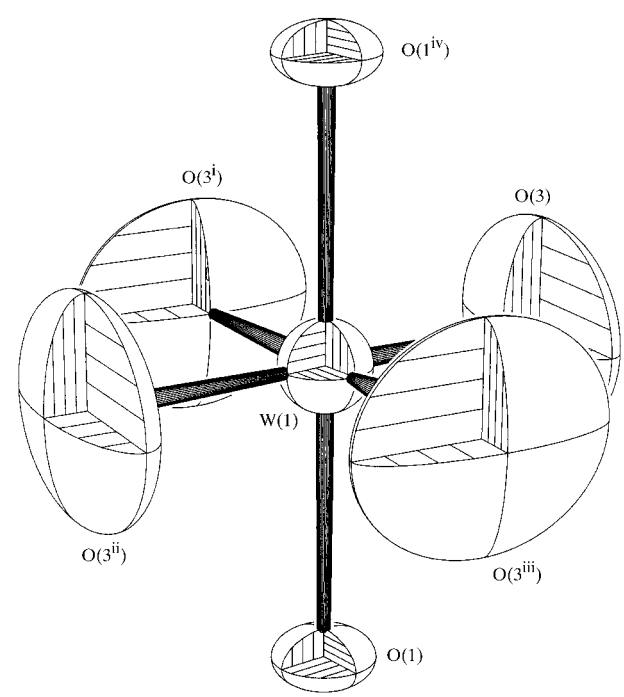

Fig. 5. *ORTEP*-3 (Farrugia, 1998) plot (ellipsoid probability 50%) showing the coordination environment of W atoms in the final refined structure of $Bi_{14}WO_{24}$. Symmetry codes: (i) $-y, x, z$; (ii) $-x, -y, z$; (iii) $y, -x, z$; (iv) $-x, -y, -z$.

Table 4. *Final Rietveld-refinement statistics for $Bi_{14}WO_{24}$ and $Bi_{14}MoO_{24}$*

	Histogram	R_{wp}	R_p	$R(F^2)$	χ^2
$Bi_{14}WO_{24}$	30–130 ms	0.0598	0.0509	0.1365	
	100–200 ms	0.0822	0.0741	0.1342	
	145°	0.0512	0.0631	0.1279	
	Overall	0.0605	0.0589		7.362
$Bi_{14}MoO_{24}$	35°	0.0266	0.0383	0.0703	
	90°	0.0224	0.0337	0.0876	
	145°	0.0349	0.0474	0.0239	
	Overall	0.0246	0.0387		6.693

Table 5. *Bond-valence sums (Brese & O'Keeffe, 1991) for the final Rietveld-refined structures of $Bi_{14}WO_{24}$ and $Bi_{14}MoO_{24}$*

Atom	$Bi_{14}WO_{24}$	$Bi_{14}MoO_{24}$
Bi(1)	2.96	2.96
Bi(2)	3.19	3.28
Bi(3)	2.67	2.83
W(1)/Mo(1)	5.94	6.17
O(1)	1.22	1.13
O(2)	2.01	2.05
O(3)	2.11	2.05
O(4)	2.09	2.12
O(5)	2.10	2.11

fluorite-type subcell reflections, yet it appears that the majority of these are accounted for by small displacive modulations of those atoms remaining in pseudo-fluorite-type positions. The fact that a fully ordered model containing WO_4 tetrahedra could be proposed with only minor symmetry lowering (from $I4/m$ to $I\bar{4}$) strongly suggested such a model at the outset; however, insufficient evidence could be found in the observed data. While it is possible that some of the disorder is a consequence of slight compositional inhomogeneities, the sharpness of the observed reflections is such that it still ought to be possible to refine a more ordered model (with larger atomic displacement parameters) if such order truly existed. The observation of such partial ordering for $Bi_{14}WO_{24}$ and $Bi_{14}MoO_{24}$ will be useful in our subsequent investigations of the crystal structures of other fluorite-related bismuth-rich phases in binary oxide systems.

The authors gratefully acknowledge the assistance of the Access to Major Research Facilities Programme and Dr Ron Smith, ISIS, in the collection of neutron powder diffraction data.

References

Allnat, A. R. & Jacobs, P. W. M. (1961). *Proc. R. Soc. London Ser. A*, **260**, 350–369.
Allnat, A. R. & Jacobs, P. W. M. (1967). *Chem. Rev.* **67**, 681–705.
Brese, N. E. & O'Keeffe, M. (1991). *Acta Cryst.* B**47**, 192–197.
Egashira, M., Matsuo, K., Kagawa, S. & Seiyama, T. (1979). *J. Catal.* **58**, 409.
Farrugia, L. J. (1998). *ORTEP-3 for Windows*. University of Glasgow, Scotland.
Gattow, G. & Schröder, H. (1962). *Z. Anorg. Allg. Chem.* **318**, 176–189.
Harwig, H. A. (1978). *Z. Anorg. Allg. Chem.* **444**, 151–166.
Hull, S., Smith, R. I., David, W. I. F., Hannon, A. C., Mayers, J. & Cywinski, R. (1992). *Physics*, B**180&181**, 1000–1002.
Ibberson, R. M., David, W. I. F. & Knight, K. S. (1992). *The High Resolution Powder Diffractometer (HRPD) at ISIS - A User Guide.* Report RAL-92–031. Rutherford Appleton Laboratory, Chilton, Didcot, England.
Larson, A. C. & Von Dreele, R. B. (1991). *GSAS. The General Structure Analysis System.* Los Alamos National Laboratory, Los Alamos, USA.
Ling, C. D., Withers, R. L., Schmid, S. & Thompson, J. G. (1998). *J. Solid State Chem.* **137**, 42–61.
Sleight, A. W. (1980). *Science*, **208**, 895–900.
Takahashi, T. & Iwahara, H. (1978). *Mater. Res. Bull.* **13**, 1447–1453.
Von Dreele, R. B. (1990). Unpublished work.
Zhou, W. (1994). *J. Solid State Chem.* **108**, 381–394.